

INTENSE L-BAND ELECTRON LINAC FOR INDUSTRIAL APPLICATIONS*

B. Park[#], S. H. Kim, S. I. Moon, J. S. Oh, S. J. Park, M. H. Cho and W. Namkung,
POSTECH, Pohang 790-784, Korea

Abstract

An intense L-band travelling-wave electron linac is under development for irradiation applications. It is capable of producing 10 MeV electron beams of 30 kW average beam power. The operating energy is limited to prevent neutron production. On the other hand, the current is limited by the beam loading effect in the given structure. The accelerating structure operated with $2\pi/3$ mode is constant-impedance and disk-loaded waveguides. We determined the optimum operating parameters by adjusting the duty factor, which is again governed by the available high-power pulsed klystron. The SUPERFISH code was used to design the bunching and accelerating cavities. The PARMELA code gives the result of beam dynamics. We present design details of the intense travelling-wave linac powered by a 1.3 GHz, 25 MW pulsed klystron with a duty factor of 2.1×10^{-3} . We also present cold test results for the prototype cavities.

INTRODUCTION

There are growing demands for the industrial application of the electron linac system [1]. Most of medical applications require 10 to 20 MeV low-current, low-repetition rate system. Other applications such as high energy X-ray generation for the container inspection require ~ 9 MeV, medium current, ~ 200 pps linac system [2], [3]. However, environmental applications such as DeSOX and DeNOx process and the sterilization process require relatively high average beam power which will depend upon the process speed.

We are developing a high-average power electron accelerator for the grain sterilizing industrial applications by the institutional collaboration between the Korea Accelerator and Plasma Research Association (KAPRA) and Pohang Accelerator Laboratory (PAL) at POSTECH. The accelerator is required to provide an average beam power of 30 kW at the beam energy of 10 MeV. In order to achieve the beam power, we adopted a travelling-wave $2\pi/3$ mode and a constant impedance accelerating structure at an operating frequency of 1.3 GHz. The accelerating structure includes a bunching section at the beam entrance. The configuration was determined using the PARMELA code. RF cavities were designed using the SUPERFISH code. For actual fabrication, we conducted RF cold tests.

The accelerator parameters are described in the next section followed by the results of the cold tests for the RF cavity structure.

*Work supported by KAPRA and PAL
[#]gobjnej@postech.ac.kr

ACCELERATOR SYSTEM

The accelerator uses an RF frequency of 1.3 GHz. The lower frequency gives two advantages: increase of the aperture limitation and reduction of the space charge effect between beam-bunches. The summary of the essential accelerator parameters are listed in the Table 1.

Table 1: Accelerator Parameters

RF System Parameter	
Operating Frequency	1.3 GHz
Pulsed RF Power	25 MW
Pulse Length	7 μ s
Repetition Rate	350 Hz
Averaged RF Power	60 kW
E-gun Parameter	
High Voltage	80 kV
Pulsed Beam Current	1.6 A
Pulse Length	6 μ s
Repetition Rate	350 Hz
Beam Parameter	
Pulsed Beam Current	1.45 A
Beam Transmission Rate	91%
Averaged Beam Power	31.4 kW
No Loaded Beam Energy	17 MeV
Accelerating Structure Parameter	
Type of Structure	Constant-impedance
Shape of Cell	Disk-loaded
Operating Mode	$2\pi/3$ mode
RF Filling Time	0.8 μ s
Operating Temperature	$40^\circ\text{C} \pm 1^\circ\text{C}$
Averaged Accelerating Gradients	4.2 MV/m

The RF system provides a peak power of 25 MW to the accelerating column and the pre-buncher. The RF pulse length is 7 μ s with the repetition rate of 350 Hz.

The E-gun has a thermionic cathode, and it will be operated by 80 kV pulses. The optimum emission current from the E-gun is set at 1.6 A. The pulse length of the beam is 6 μ s, since the RF filling time of the accelerating structure is 0.8 μ s.

The accelerating structure is a disk-loaded waveguide. It is a constant-impedance structure operated with a $2\pi/3$ mode traveling wave. This structure satisfies the fully beam-loaded condition. With simulations by the

SUPERFISH and the PARMELA codes, it is confirmed that this accelerator is capable of satisfying the design goals. If the system is operated at the negligible beam loading condition, the accelerator can produce 17 MeV electron beams.

The accelerator system is consisted of the klystron system, the waveguide network, a prebuncher, an accelerating column, and a beam scanner system. Overall layout of the system is shown in Figure 1. The klystron system is consisted of the Thales TV2022D klystron and the matching pulsed modulator. Due to high average power requirement, total 8 units of 30-kW high-voltage inverter stack connected in parallel will be used for the PFN charging. The waveguide network is consisted of straight waveguides, and special waveguide components will be filled with SF₆ gas. Two sets of high power ceramic windows are used for the vacuum break at the input and output couplers of the accelerating column. A 33-dB cross-coupled directional coupler (CXDC) is inserted in the waveguide network for the prebuncher cavity.

In order to keep vacuum condition for the beamline components, 3 ion pumps are required. The ion pump 1 (20 l/s) is for the E-gun, ion pump 2 and 3 (240 l/s) are for the accelerating column and the beam scanner.

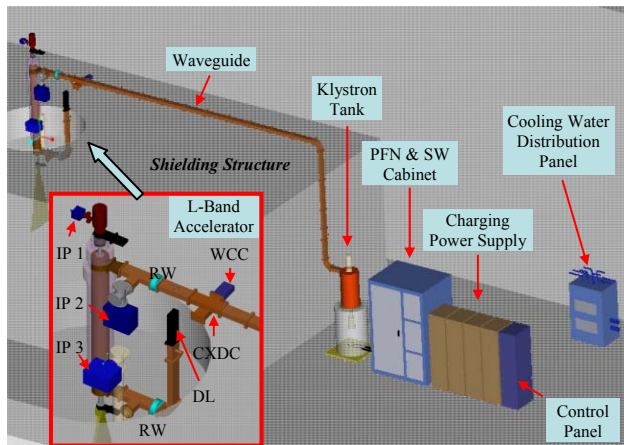


Figure 1: Layout of the accelerator system (IP: Ion Pump, RW: RF Window, DL: Dummy Load, WCC: Waveguide to Coax Converter, CXDC: Cross-coupler Directional Coupler).

COLD TESTS

Resonant Frequency

On the machine parameters determined by simulations, we conducted RF cold tests with aluminium test cavities. To measure the resonant frequency at $2\pi/3$ mode, the test-cavity consists of 2 cells and 2 half-cells (or 1 cell and 1-half cell). The RF signal is measured by a monopole antenna and analyzed with the network analyzer, Agilent E8362B. Table 2 shows the measured resonant frequencies for test-cavities, and they are all within tuneable ranges using tuning holes fabricated at the side wall of each cavity.

Table 2: Resonant Frequency at $2\pi/3$ Mode

Cavity	Resonant Frequency (MHz)
Main Cell	1299.480
2 nd buncher	1297.620
3 rd buncher	1298.220
4 th buncher	1298.220
5 th buncher	1298.100

Impedance Matching for Input and Output Coupling Cavities

The test for the input and output coupling cavities is based on the Kyhl's method [4]. According to this method, phase shifts for three frequencies due to the movement of a shorting bar indicate the strength of coupling. Three frequencies are $\omega_{\pi/2}$, $\omega_{2\pi/3}$, and ω_m , where, $\omega_{\pi/2}$ and $\omega_{2\pi/3}$ are the resonant frequencies in the second cavity for $\pi/2$ and $2\pi/3$ modes, respectively. The ω_m is the mean value of $\omega_{\pi/2}$ and $\omega_{2\pi/3}$. If the coupling cavity is critically coupled, the phase shift of $\omega_{\pi/2}$, ω_m , and $\omega_{2\pi/3}$ should be 120° , 180° , and 240° , respectively, when the shorting bar moves from the center of the coupling cavity to the center of the second cavity. For the impedance matching between the waveguide system and the coupling cavity, the size of the coupling hole and the coupling cavity radius are adjusted by careful iterative machining. Figure 2 shows the experimental setup for the impedance matching for input and output coupling cavities.

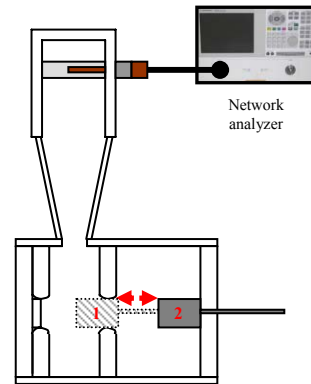


Figure 2: Measurement setup.

When the shorting bar is at the position 2 in Figure 2, we measure the resonant frequency ω_c . And we find two frequencies: $\omega_1 = \omega_c - \delta\omega$ and $\omega_2 = \omega_c + \delta\omega$, where, $\delta\omega = (\omega_{2\pi/3} - \omega_{\pi/2})/2$. The coupling coefficient β is calculated by Equation (1) with measured reflected angles, ϕ_1 and ϕ_2 for two frequencies, ω_1 and ω_2 .

$$\beta = \frac{1}{\frac{k}{2} \omega_{\pi/2} \sin \frac{2\pi}{3}} \cdot \frac{\tan \frac{\phi_1}{2} \tan \frac{\phi_2}{2} (\omega_1^2 - \omega_2^2)}{\tan \frac{\phi_2}{2} \omega_1 - \tan \frac{\phi_1}{2} \omega_2} \quad (1)$$

We may also define $\Delta\omega_c = \omega_c - \omega_m$ which should be zero in the critical coupling case.

In actual tuning process, the starting value of the coupling aperture dimension is based on the result from SUPERFISH simulation. The width of coupling aperture was fixed as 27 mm. The input and output coupling cavity radii were also fixed as 88.58 and 88.85 mm, respectively.

Figure 3 and 4 show the results of input and output coupler tuning measurements, as we progressively making the aperture length larger by careful matching. In the figures, $f_{\text{res}} = (\omega_c/2\pi)$ is the resonant frequency. As the coupling aperture length increases, the resonant frequency decreases, and β increases. The resonant frequency is close to the mean frequency near the input coupler radius of 69.5 mm and the output coupler radius of 74.5 mm. For the input coupler cavity, the mean frequency ω_m is 1294.757 MHz ($\Delta\omega_c = 0.107$ MHz). For the output coupler cavity, the mean frequency ω_m is 1297.5 MHz ($\Delta\omega_c = -0.050$ MHz). At the smaller aperture length, the resonant frequency has higher value and the coupling is under-coupled ($\beta < 1$). At the longer aperture length, it represents the lower resonant frequency and over coupling ($\beta > 1$).

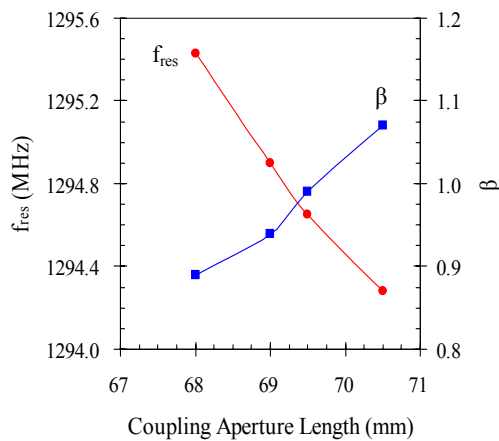


Figure 3: Result of input coupler test.

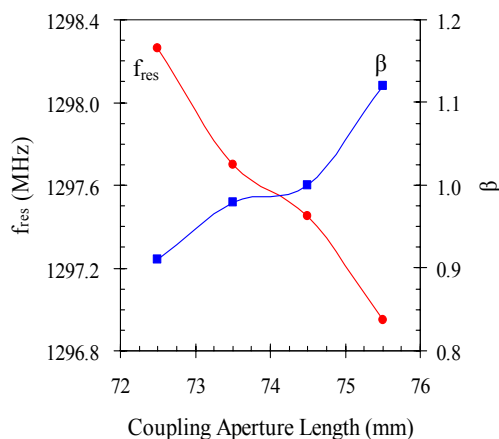


Figure 4: Result of output coupler test.

SUMMARY

We designed an intense L-band travelling wave electron linac of 10 MeV and 30 kW for the sterilizing industrial application. The cavity dimensions for the $2\pi/3$ mode travelling wave were designed by SUPERFISH simulations. We described the detailed procedure for the determination of the final fabrication dimensions of the coupling cavities. The apertures of the coupling cavities are very important for the accelerator performance. We conducted RF cold tests which required an iterative process of fine geometrical adjustments of the apertures for the matched condition. In the tuning process, we observed a change from under-coupled to over-coupled conditions, when we pass through the right resonance frequency. This work will be progressed to the manufacturing of the accelerating structure. All other components, fabrications are also underway for the completion of the intense L-band linac system.

ACKNOWLEDGMENTS

The authors appreciate Dr. Luo Yingxiong at IHEP, Beijing for useful discussions and Mr. Y. J. Park for the cavity fine machining. This work was supported by Korea Accelerator and Plasma Research Association (KAPRA) and Pohang Accelerator Laboratory (PAL).

REFERENCES

- [1] A. M. M. Todd, "Emerging Industrial Applications of Linacs," in *Proc. Int. Linac Conf.* (Chicago, IL, Aug. 23-28, 1998), 1036 (1998).
- [2] V. L. Auslender, "5-10 MeV Industrial High Power Electron Accelerators," in *Proc. Int. Linac Conf.* (Gyeongju, Korea, Aug. 19-23, 2002), 284 (2002).
- [3] V. Pirozhenko et al., "Complex for X-ray Inspection of Large Containers," in *Proc. 2006 EPAC* (Edinburgh, Scotland, June 26-30, 2006), 2388 (2006).
- [4] E. Westbrook, Microwave Impedance Matching of Feed Waveguides to the Disk-Loaded Accelerator Structure Operating in the $2\pi/3$ Mode, SLAC-TN-63-103 (1963).
- [5] S. Zheng, Y. Cui, H. Chen, L. Xiao, "A Quantitative Method of Coupler Cavity Tuning and Simulation," in *Proc. 2001 PAC* (Chicago, IL, June 18-19, 2001), 981 (2001).